4th International Conference on Structural Health Monitoring of Intelligent Infrastructure (SHMII-4) 2009
22-24 July 2009, Zurich, Switzerland

Vibration characteristics of a damaged FRP vehicle bridge

Johanna C. Landherr [1], Mark F. Green [1], R. Gordon Wight [2], and Marie-Anne Erki [2]

[1]Queen's University, Kingston, Ontario, Canada
[2]Royal Military College of Canada, Kingston, Ontario, Canada

ABSTRACT: The 9.6 m pultruded glass fiber reinforced polymer (FRP) deployable box beam presented in this paper is one of the tracks of a two track military vehicular bridge, designed to aid cross-country mobility in areas where infrastructure has been damaged by conflict or natural disasters. Finite element analysis was validated for the undamaged box beam by quasi-static and dynamic testing in the laboratory and in the field, and was used to analyze the potential damages to the box beam that would not be otherwise easily detected by eye. The changes in vibration characteristics for the damaged FRP box beam, specifically the first natural frequency and mode shape curvatures, are presented. Laboratory testing of the undamaged and progressively damaged FRP box beam is described, and those results will be presented at the conference. The challenges of identifying types of damage and their severity based on a change in vibration characteristics are discussed.

1 INTRODUCTION

1.1 Design of the FRP box beam

Pultruded glass fiber reinforced polymer (FRP) can be used to advantage for certain types of bridges and bridge components, such as lightweight footbridges, military emergency bridges, and bridge deck replacements. Based on the experience gained from the construction and testing of a 4.8 m FRP box beam (Wight et al., 2006), a 9.6 m FRP double track deployable bridge was designed by the "Concrete/FRP Structural Research Group" at the Royal Military College of Canada (RMC). The goal of this design is to provide a gap crossing aid for enhanced cross-country mobility of wheeled military vehicles, where there are no roads, or where roads have been damaged. Its design was based on the Military Load Class 30 (MLC 30), a NATO (2006) vehicle class, which includes a wheeled vehicle of 30.84 tonnes and a tracked vehicle of 27.22 tonnes.

Each track of the bridge is a box beam that is 1.22 m wide, 9.6 m long, and is tapered with a maximum height at mid-span of 0.953 m, with two slopes on either side of the apex, giving the top plate an angle of 11.7º at the supports and 8.4º at 2400 mm from the supports. This two-step angle change reduces the total change in angle at mid-span, thereby reducing the impact force effect caused by a vehicle going over the apex. Only one of the two box beams for the double

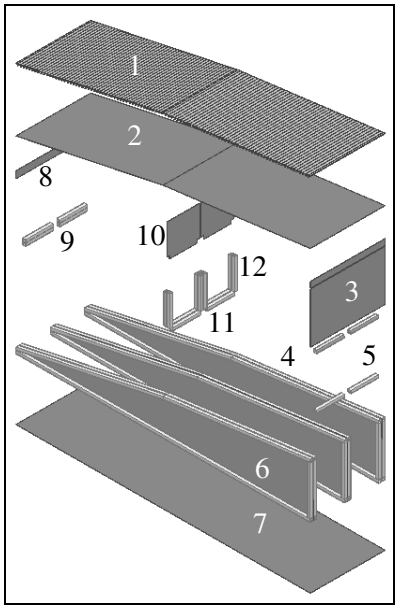

Figure 1. Components of half of the box beam: 1-ribbed decking; 2- top plate; 3-mid-span diaphragm; 4-mid-span diaphragm transversal tube (upper); 5-mid-span diaphragm transversal tube (lower); 6-beams; 7-bottom plate; 8-end cover plate; 9-end transversal tube; 10-quarter-span diaphragm; 11-quarter-span diaphragm transversal tube; and 12-quarter-span diaphragm vertical tube.

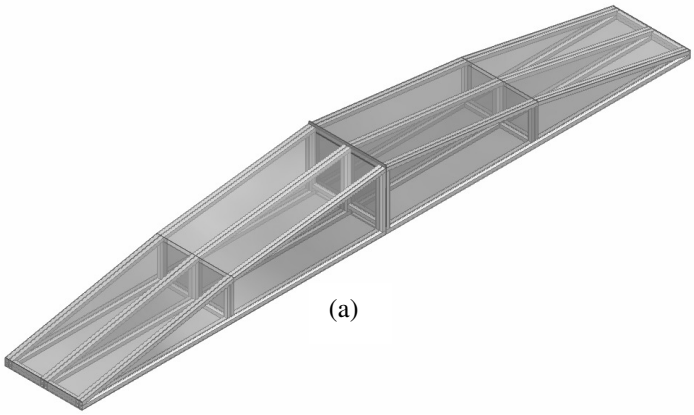

(a)

(b)

Figure 2. FRP box beam (a) translucent model; (b) Bison vehicle testing set-up.

track bridge was fabricated for testing. It was built in two pieces, connected at midspan by a steel hinge, with hinge plates 300 mm × 1220 mm. Figure 1 shows the components of the box beam. All the FRPs used in the box beam were purchased from Creative Pultrusions Incorporated (2000). The fibers were E-glass, and the materials had alternating layers of unidirectional fibers and random fiber mats. The sections used were 1625 series (thermoset vinyl ester class 1 FR) for the 51 mm × 51 mm × 6.4 mm rectangular tubes, 1625 series 6.4 mm flat sheets for the webs, top and bottom plates and internal diaphragms, and 40 mm thick ribbed decking Flowgrip Flooring panel for the wearing surface. A polyurethane structural adhesive was used throughout to bond the sections, thereby avoiding the stress concentration problem of bolted connections. The box beam has a total mass of approximately one metric tonne. Figure 2a and 2b show, respectively, a semi translucent model of the box beam and the box beam set-up for the vehicle tests, with a gravel ramp built beside it, standing in for the second FRP box beam.

1.2 Dynamic testing of the undamaged box beam

Most bridge dynamic testing programs focus on measuring the natural frequencies and damping of the structure. The FRP box beam was tested initially in its undamaged state to determine its static and dynamic behaviors, which confirmed that it is structurally adequate for the MLC 30 design load (Xie et al., 2008; Landherr, 2008). Dynamic testing was done both in the laboratory

using an instrumented hammer (Xie, 2007) and in the field using three different types of military vehicles (Landherr, 2008).

Vehicle tests were first conducted using a Bison, which is an eight-wheeled armored personnel carrier of MLC 16. In the field testing, one line of wheels traversed the FRP box beam and the other drove on the gravel ramp (Figure 2b). Displacements, strains, and accelerations were collected at selected points on the box beam. To test the box beam's dynamic performance, the Bison crossed the bridge at speeds varying from 10 km/h to 25 km/h. To induce additional dynamic impact, a wood beam (100 mm by 100 mm) was placed on the west half of the box beam and gravel ramp, approximately 0.30 m from mid-span. Additional tests were conducted with the vehicle braking hard after the front two wheels crossed mid-span. Tests were also conducted with two other types of military vehicles to evaluate the response of the box beam to different types of a) vehicle suspension, b) vehicle loads, and c) number of wheels per track. The first vehicle, a Heavy Logistic Vehicle Wheeled (HLVW), is a cross between a flatbed transport truck and an all terrain vehicle. The total mass of the HLVW is 15,000 kg, similar to the Bison, but with only six wheels and a different suspension system. The second vehicle, a 25,500 kg forklift, was used for quasi-static testing. The vehicle could be driven in either direction, either leading with the counterweight or with the forks. In the Bison and HLVW vehicle tests, the accelerometers were sampled at 4800 Hz and the strain gauges and LVDTs at 1200 Hz. For the forklift tests, all instrumentation was sampled at 50 Hz due to the slow speed of loading used for these tests. Additional details about these tests will be given in other papers.

The first natural frequencies calculated from the instrumented hammer tests and the vehicle tests were nearly equal (between 11 and 12 Hz), and unlikely to evoke resonance, since a moving vehicle may have a natural frequency of 2 to 3 Hz. From the instrumented hammer tests, the measured damping ratio of the first frequency was calculated to be 3.3%.

2 VIBRATION CHARACTERISTICS OF DAMAGED STRUCTURES

This paper reports on the changes in the first natural frequency and mode shape curvatures for the FRP box beam subjected to damage of various degrees and types. The mode shape curvature analysis is a vibration-based damage detection method that has been used for machine parts, and with varying success for civil engineering structures (Xiang and Yang, 2004; Mikami et al., 2004; Sarazin and Newhook, 2004). It was chosen for the FRP box beam because the results obtained when the undamaged box beam was tested using both an instrumented hammer and three different vehicles were relatively easy to interpret. Also, the hammer and vehicle tests of the undamaged box beam yielded such similar results that the choice of laboratory or field testing of the damaged box beam could be determined by convenience.

Most studies of vibration-based damage detection have been conducted for obvious structural component damages, such as removal of pieces of the structure. While interesting as a first examination of such questions, it is unlikely to be used in practice to discover the obvious. Hence, for this study, detection by the mode shape curvature analysis of visible damage to components, such as FRP tension failures, was avoided. However, previous testing of a smaller 4.8 m box beam (Wight et al., 2006) revealed that the types of failures that occurred due to overloading were not initially easily detected by eye, these being debonding of the top plate, crushing of the ribbed decking bonded to the top plate, and buckling of the webs. Therefore, these were the types of damage considered in the study.

The ISIS Guidelines for Structural Health Monitoring (2001) gives the following central difference equation for the mode shape curvature as a function of the measured displacement components:

$$\frac{\phi_i^{k+1} - 2\phi_i^k + \phi_i^{k-1}}{h^2} \tag{1}$$

where k-1, k, and k+1 denote locations of displacement measurements, X_{k+1}-X_k=X_k-X_{k-1}=h and ϕ_i^k is the modal displacement at location k in mode number i.

As Wegner et al. (2004) pointed out, vibration-based damage detection methods for structural health monitoring of civil engineering structures is complicated, because of the large size of structures, the variability of their material properties, support conditions, and connectivity of their components, as well as the variability in loading and environmental conditions. Fortunately, the FRP box beam is a relatively small structure that was built by skilled labor, in a well supervised setting, using materials manufactured under good quality control, and connected throughout by carefully produced bonded joints. The support conditions were simple and could be controlled for all tests, and, for the most part, the testing was done in ideal environmental conditions. Therefore, it is not surprising that the data obtained from the static and dynamic tests could be easily interpreted, and that the first natural frequency obtained in the laboratory was confirmed by the vehicle testing. The pitfalls that plague data interpretation gathered in bridge testing, as discussed by Bakht (2004), were mostly avoided in these ideal conditions.

Also, although FRP is an anisotropic material, it has linear elastic behavior to failure, and the results of the finite element analysis of the structure were easily validated by the test data (Xie, 2007; Landherr, 2008). Therefore, the changes in mode shape curvature for the damaged FRP box beam were first studied using finite element modeling, and these are presented in this paper. A three dimensional model of the box beam was constructed in SAP2000 (2008), using 4-noded shell elements for all the plates and 2-noded beam elements for the square tubes. The moduli of elasticity for all the 6.4 mm flat sheets in their lengthwise and crosswise directions were 17.2 GPa and 12.2 GPa, respectively (lengthwise being in the direction of the unidirectional fibers). The material behavior of the square tubes was assumed to be uniaxial, with a modulus of elasticity of 28.6 GPa. Laboratory testing to validate the analyses is ongoing and its results will be presented at the conference.

2.1 Debonding of the top plate

Debonding damaged was studied by Sarazin and Newhook (2004), who used strain readings and vibration analysis to identify structural debonding of carbon fiber reinforced polymer (CFRP) sheets bonded to the tensile face of reinforced concrete beams as external strengthening. However, owing to the overall small contribution of the CFRP sheets to the stiffness of the beams, Sarazin and Newhook concluded that strain values are more promising than stiffness or modal values for identifying this type of damage.

However, the top plate of the FRP box beam is a major structural component (component 2 in Figure 1), carrying a significant portion of the compressive stresses of the box beam. Its debonding was modeled by detaching it at the quarter span diaphragm (component 10 in Figure 1) located at 2400 mm from the left support. This debonding pattern was chosen, because in the 4.8 m box beam debonding was observed at its quarter span diaphragm. In the three debonding cases considered, as described below, debonding was assumed to have occurred over the entire width of the box beam. In the first debonding analysis, the top plate was debonded over a length of 1.2 m, which was comprised of two 0.6 m lengths on both sides of the internal diaphragm. For the second debonding analysis, the debonded length extended another 0.6 m toward the left support, for a total debonded length of 1.8 m. For the final debonding analysis, the debonding of the top plate was extended all the way to the left support for a total debonded length of 3.0 m.

The first natural frequency of the box beam, undamaged and damaged by debonding of the top plate over the lengths 1.2 m and 1.8 m remained unchanged at 12.4 Hz, but decreased to 11.7 Hz when the debonding extended to the support, reaching a length of 3.0 m. Even in the ideal testing conditions of the FRP box beam, it would not be realistic to conclude that a measured difference of less than 1 Hz would be due to debonding and not to some other external influence.

However, the mode shape curvature analysis yields some striking results, as shown in Figure 3. The locations of the debonded lengths are shown. The mode shape curvatures for the 1.2 m and 1.8 m debonded lengths are nearly identical to that of the undamaged box beam, with only very little differences in the box beam half where the debonding was induced and none at all in the other half. With a 3.0 m debonded length from the left support, the mode shape curvature shows significant departure from that of the undamaged box beam, particularly to the left of the midspan (x = 0), where the debonding was induced. It also shifted the values of the mode shape curvatures in the second half of the box beam, where there is no debonding, although the general shape of the curvatures remains unchanged in this zone.

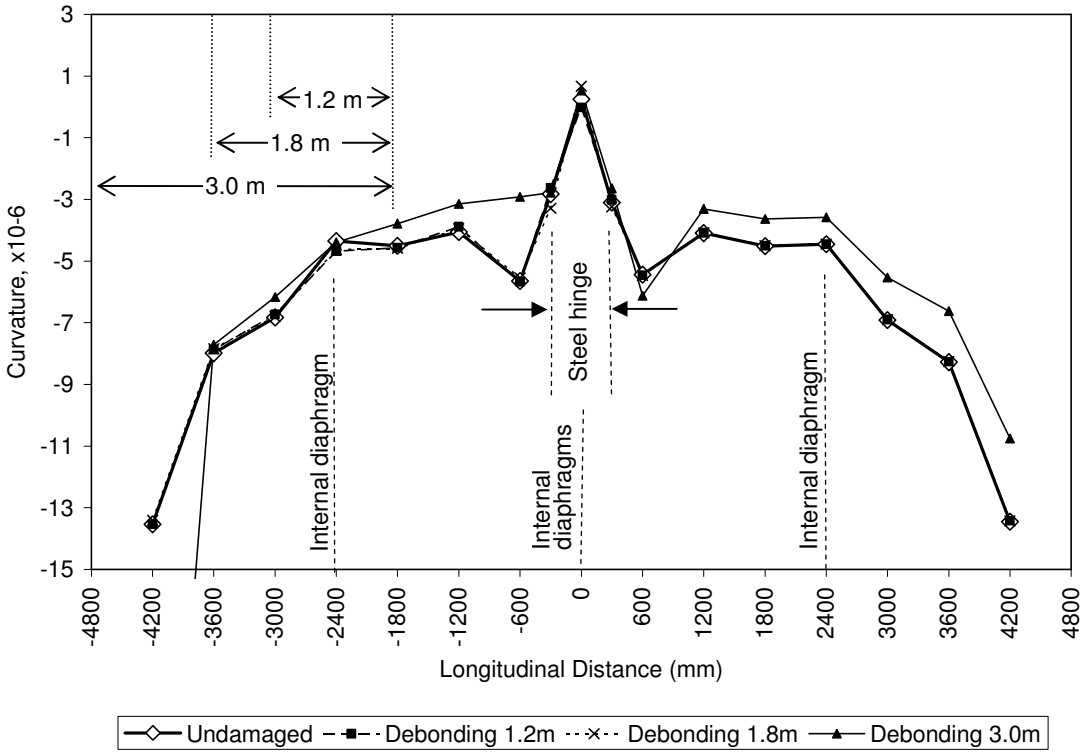

Figure 3. Mode shape curvatures for the box beam undamaged and damage by debonding of the top plate.

2.2 *Crushing of ribbed decking*

The ribbed decking (component 1 in Figure 1) was assumed crushed over lengths denoted as AB, ABC, and ABCD in Figure 4, these being 0.6 m, 1.2 m, and 1.8 m, respectively. The crushing over these lengths was further assumed to be over the entire width of the box beam, as being the most severe case. While crushing of the ribbed decking can be heard if it occurs while the box beam is being observed, it is not easily detected by a cursory inspection of the box beam or by vehicle occupants when the box beam is being crossed.

The first natural frequencies of the box beam, undamaged and damaged by crushing of the ribbed decking over the three increasing lengths, were 12.39 Hz, 12.34 Hz, 12.46 Hz, and 12.48 Hz, respectively, or for all practical purposes identical.

The mode shape curvature analysis, summarized in Figure 4, revealed distinct departures from the mode shape curvature of the undamaged beams in the zones where the crushing was induced. Therefore, when crushing of the ribbed decking was over the length AB, the mode shape curvature of the damaged structure was different from that of the undamaged structure predominantly between points A and B. When the crushing was over ABC, the mode shape curvature was offset from that of the undamaged structure over points A, B, and C. A similar observation can be made for crushing over the length ABCD, with the inset given in the upper left hand corner of the graph showing these trends more clearly.

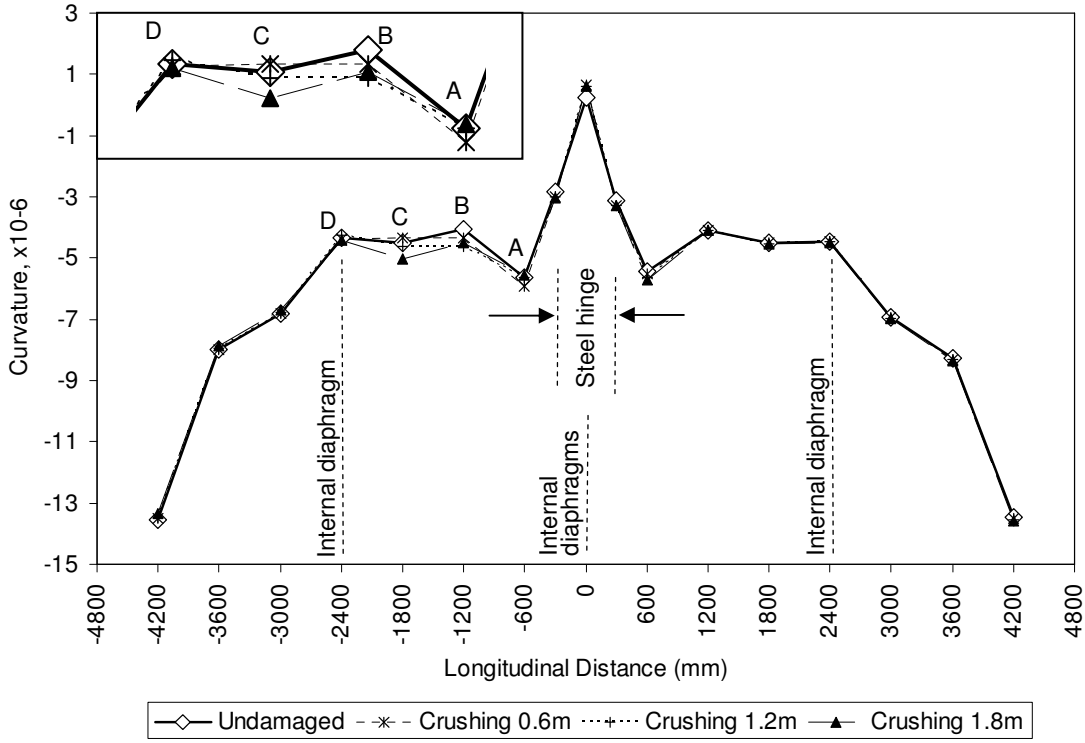

Figure 4. Mode shape curvatures for the box beam undamaged and damage by crushing of the ribbed decking.

2.3 Buckling of the web of the interior beam

The web of the interior beam (component 6 in Figure 1) was assumed buckled due to wheel loading over lengths 0.6 m and 1.2 m. The web of the interior beam was chosen for the damage detection, because the interior beam is encased in the box beam and damage to it is not visible.

The first natural frequencies of the box beam, undamaged and damaged by buckling of the interior web over lengths 0.6 m and 1.2 m were 12.39 Hz, 12.37 Hz, and 12.36 Hz, respectively, or for all practical purposes identical.

The mode shape curvature analyses, summarized in Figure 5, show patterns for the damaged box beam due to web buckling that are distinct from the top plate debonding (Figure 3) and ribbed deck crushing (Figure 4) damages. The mode shape curvatures of the damaged box beam

deviated from those of the undamaged structure at the locations where the interior beam web buckled.

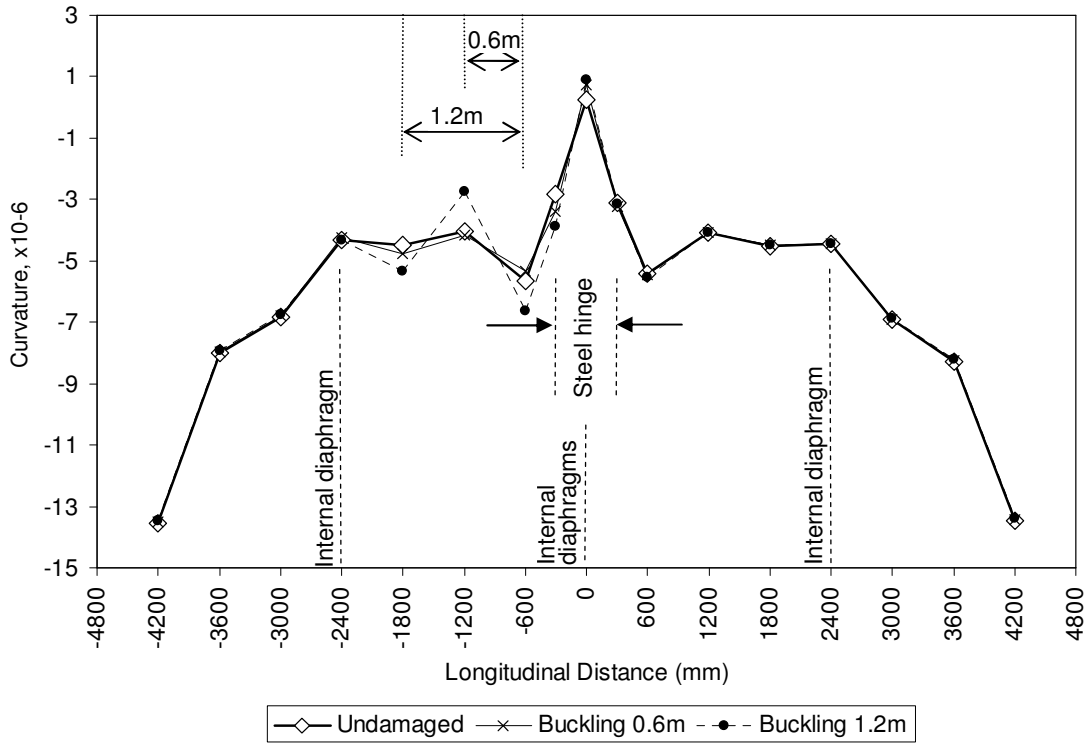

Figure 5. Mode shape curvatures for the box beam undamaged and damage by buckling of the internal central web.

3 VIBRATION CHARACTERISTICS DERIVED FROM LABORATORY TESTING

In the laboratory, the box beam was excited by releasing it rapidly from a deflected position imposed by an hydraulic actuator applying a load at midspan. The main components of the test were a harness that went entirely around the section of the box beam at midspan and a rapid-release hook inserted into the laboratory floor under the geometric centre of the underside of the box beam. For each test, the box beam was displaced such that the hook could be latched onto the harness. The actuator was raised, and the box beam was held down in its deflected shape by the hook. (The actuator had to be raised sufficiently to prevent interference with the impending box beam response.) When the hook mechanism was released, the box beam vibrated freely through many cycles. Displacements, strains, and accelerations were recorded. While strain readings may not always be the most practical type of instrumentation for field testing, herein they were more reliable than displacement readings for calculating the mode shape curvatures. Indeed, Sarazin and Newhook (2004) showed that strain measurements can be more indicative of component damages than changes in natural frequencies, and Mufti et al. (2007) demonstrated how strain gauges readings can be used to calculate displacements, as a backup for the displacement measurements. The box beam was tested with different support conditions in an undamaged state and was then progressively damaged. The results will be presented at the Conference, but suggest that even in nearly ideal conditions tracking damage using vibration characteristics is difficult, because very small differences in measurement readings can greatly affect calculated vibration characteristics.

4 CONCLUSIONS AND RECOMMENDATIONS

Before mode shape curvatures can be used for damage identification, the types of damage likely to occur in a structure should be defined. In the box beam, debonding of the top plate, crushing of the ribbed decking, and buckling of the beam webs were the three main types of damage anticipated. Mode shape curvatures for these types of damage appeared to have distinct traits or "signatures". Therefore, modeling of the structure may predict the mode shape curvature changes expected for the different damage types. However, since one type of damage can precede and initiate other types of damage, and with infrequent periodic testing of the structure, several damage types may be concurrently present. Finding a means of decoupling superimposed mode shape curvature plots could be helpful in identifying multiple damage types.

For the types of damages assumed in this study, which do not consist of obvious removal of structural components, the changes in first natural frequency were quite small, even when these damages extended over a significant portion of the box beam. Therefore, it would be difficult to identify damage early or to attribute changes in first natural frequency measured in the field to a particular type of damage.

5 REFERENCES

Bakht, B. 2004. Interpretation of data: a major obstacle in SHM of bridges (Keynote Paper). Proceedings of the Second International Workshop on Structural Health Monitoring of Innovative Civil Engineering Structures, ISIS Canada Research Network, Winnipeg, Canada, pg. 61-73.

Creative Pultrusions Inc., 2000. The New and Improved Pultex® Pultrusion Global Design Manual of Standard and Custom Fiber Reinforced Polymer Structural Profiles, Vol. 3, Rev. 3,Chapter 3, p 4-6.

Landherr, JC. 2008. Dynamic analysis of a FRP deployable box beam. MSc Thesis in the Department of Civil Engineering, Queen's University, Kingston, Ontario, Canada, 113 pg.

Mikami, S, Beskhyroun, S, Miyamori, Y, Oshima, T. 2007. Application of a vibration-based damage detection algorithm on a benchmark structure. The 3rd International Conference on Structural Health Monitoring of Intelligent Infrastructure Vancouver, British Columbia, Canada.

Mufti, AA, Jaeger, L, Klowak, C, Bakht, B, and Tadros, G. 2007. Calculating deflections from observed strains. The 3rd International Conference on Structural Health Monitoring of Intelligent Infrastructure Vancouver, British Columbia, Canada.

NATO 2006. Military Load Classification of Bridges, Ferries, Rafts and Vehicles, STANAG 2021.

SAP2000. 2008. Structural Analysis Program, Computers and Structures, Berkeley, California.

Sarazin, GA, Newhook, J. 2004. Detection of debonding damage in CFRP strengthened concrete beams. Proceedings of the Second International Workshop on Structural Health Monitoring of Innovative Civil Engineering Structures, ISIS Canada Research Network, Winnipeg, Canada pg. 361-379.

Wegner, LD, Zhou, Z, Alwash, M, Siddique, AB, Sparling, BF. 2004. Vibration-based damage detection on bridge superstructures. Proceedings of the Second International Workshop on Structural Health Monitoring of Innovative Civil Engineering Structures, ISIS Canada Research Network, Winnipeg, Canada pg. 429-440.

Wight, RG, Erki, MA, Shyu, CT, Tanovic, R, Heffernan, PJ. 2006. Development of an FRP Short Span Deployable Bridge. ASCE Bridge Journal, Vol. 11, No. 4, pp. 489-498.

Xiang, YQ, Yang, WL. 2007. Damage identification of the multi-box girder bridge by modal curvature methods. The 3rd International Conference on Structural Health Monitoring of Intelligent Infrastructure Vancouver, British Columbia, Canada.

Xie, A, Wight, RG, Erki, MA. 2008. Development of an FRP deployable bridge. 5th International Conference on Advanced Composite Materials in Bridges and Structures (ACMBS-V), Winnipeg, Manitoba, Canada.

6 ACKNOWLEDGEMENTS

The authors gratefully acknowledge funding from the Department of National Defence (Canada) and the Natural Sciences and Engineering Research Council of Canada. Additionally, Ms. Landherr was a Killam Fellow of the Foundation for Educational Exchange between Canada and the United States.